



# A novel route to extreme vacua: the non-evaporable getter thin film coatings

C. Benvenuti<sup>a,\*</sup>, J.M. Cazeneuve<sup>a</sup>, P. Chiggiato<sup>a</sup>, F. Cicoira<sup>a,1</sup>, A. Escudeiro Santana<sup>a</sup>, V. Johaneck<sup>a</sup>, V. Ruzinov<sup>a,2</sup>, J. Fraxedas<sup>b</sup>

<sup>a</sup>EST Division, SM Group, CERN, CH-1211 Geneva 23, Switzerland

<sup>b</sup>Institut de Ciencia de Materials de Barcelona, ICMA-B-CSIC, Campus de la UAB, 08193, Spain

## Abstract

Vacuum chambers sputter-coated with a thin film ( $\sim 1.5 \mu\text{m}$ ) of a getter material, and subsequently exposed to ambient air, have been found to recover a pumping action after “in situ” bakeout. Coatings of Ti, Hf, Zr have been initially produced and studied, followed by their binary quasi-equiatomic alloys TiHf, HfZr, TiZr. All these coatings display activation at temperatures lower than  $400^\circ\text{C}$ , as observed by means of X-ray photoelectron spectroscopy, electron stimulated desorption (ESD), pumping speed and ultimate pressure measurements. The lowest activation onset temperature, about  $200^\circ\text{C}$ , has been measured for the quasi-equiatomic TiZr alloy. A further activation temperature decrease has been achieved for TiZr based ternary alloys/compounds, which are currently being investigated. © 1999 Elsevier Science Ltd. All rights reserved.

## 1. Introduction

Hydrogen thermal outgassing from the walls of a vacuum system represents the major obstacle to achieving extreme vacua. The  $\text{H}_2$  outgassing rate is of the order of  $10^{-13} \text{ Torr l s}^{-1} \text{ cm}^{-2}$  even for properly selected and treated metal surfaces (such as those of aluminium alloys or stainless steel) and exceeds by more than two orders of magnitude the outgassing of other molecular species, namely  $\text{CH}_4$ ,  $\text{CO}$ ,  $\text{CO}_2$ .

When dealing with small and compact vacuum systems, ultimate pressure lower than  $10^{-12}$  Torr may be easily obtained by a combination of sputter-ion and Ti sublimation pumps providing a global speed of the order of  $10^3 \text{ l s}^{-1}$ . By cooling the Ti sublimation pump with liquid nitrogen, pressures even lower than  $10^{-13}$  Torr were achieved in this way [1].

Pumping long, conductance limited vacuum chambers, such as those of particle accelerators, is more

problematic. Pressures below  $10^{-12}$  Torr may be obtained only if large and linearly distributed pumping is applied. A typical example of this situation is given by the vacuum system of the large electron positron collider (LEP) at CERN, where an ultimate pressure of about  $2 \times 10^{-12}$  Torr was achieved inside 12 m long chambers made of Al alloy and pumped by a linear non-evaporable getter (NEG) strip and a sputter-ion pump of about  $50 \text{ l s}^{-1}$  nominal speed [2]. This pressure could be further reduced to about  $5 \times 10^{-13}$  Torr by increasing the pumping speed for Ar and  $\text{CH}_4$ , not pumped by getters, with the addition of five more sputter-ion pumps of the same size [3]. In this case, the resulting ultimate pressure was set by the  $\text{H}_2$  outgassing and the linear pumping speed for  $\text{H}_2$  of about  $2000 \text{ l s}^{-1} \text{ m}^{-1}$  of NEG strip [3].

In the case of LEP the NEG pump consists of a 30 mm wide St 101 strip [4], which is activated at  $750^\circ\text{C}$  by directly passing a current of 90 A. Resistive heating implies electrical insulation, which severely limits the amount of NEG strip (and therefore the available pumping speed) which may be inserted in a given volume. A much more favourable situation may be achieved by making use of a lower activation temperature NEG (namely the St 707, also produced by SAES Getters [5]) which may be passively activated during vacuum system bakeout.

\* Corresponding author. Tel.: 0041 22 7673718; fax: 0041 22 7679150; e-mail: benvenuti@cern.ch.

<sup>1</sup> Present address: Institut d'Optique Appliquée, EPFL, CH-1015 Lausanne, Switzerland.

<sup>2</sup> Visiting Research Associate from the Moscow Steel and Alloys Institute, Moscow 117936, Russia.

In this case electrical insulation is not required and a much larger amount of strip may be installed, for instance by wrapping it on a transparent stainless steel cage which is then inserted all along the vacuum chamber. Since the two NEG's provide similar linear pumping speeds and the ratio of strip to chamber surface area is now increased by a factor 20 with respect to the LEP case, a pressure in the low  $10^{-14}$  Torr range could be achieved in this way [6].

Following the evolution described above, the ultimate pressure was progressively reduced by improving the pumping efficiency (pump closer to the walls) and increasing the applied pumping speed, but the  $H_2$  outgassing remained unchanged. In order to reduce  $H_2$  outgassing, the chamber walls and the NEG pump should be tightly joined, as could be achieved by coating the whole chamber surface with a NEG thin film. After passive activation during baking, this coating would not only prevent outgassing, but would also provide surface pumping and transform the vacuum chamber from a gas source to a pump.

A study on the feasibility of NEG thin film coatings was launched at CERN at the end of 1995 [7, 8]. The present status of this study is reported below.

## 2. Selection of getter materials

During the activation of a NEG, oxygen contained in the surface oxides is dissolved in the material bulk by heating. A low activation temperature implies high oxygen diffusivity in the getter. To cope with the maximum baking temperature allowed by the mechanical properties of construction materials, activation should not require temperatures higher than  $400^\circ\text{C}$  for stainless steel or even not higher than  $200^\circ\text{C}$  for vacuum chambers made of copper or aluminium alloys.

A second important requirement is a high oxygen solubility limit to allow many activation-air exposure cycles. When making the realistic assumption that the thickness of the oxide layer formed during air exposure is 2–3 nm, a  $1\ \mu\text{m}$  thick film would present an oxygen concentration of 2–3% after 10 such cycles. The oxygen concentration could be lowered by increasing the film thickness, but to guarantee a reasonable NEG life time a solubility limit of at least 10% is desirable.

To ensure a large pumping capacity for  $H_2$  at ambient temperature and under UHV conditions the getter should provide high diffusivity and possibly a hydride phase with low dissociation pressure. Finally, the ideal material should provide large enthalpies of adsorption for all the gases which are usually present inside UHV vacuum systems, i.e.  $H_2$ , CO,  $\text{CO}_2$ ,  $\text{N}_2$ .

In addition to these properties which characterize the "vacuum behaviour", the selected getter material should also provide other essential features, namely good

adhesion to the substrate, high mechanical resistance and high melting point (to withstand cathode heating during the coating process, see Section 3). Furthermore, it should be non-toxic, non-pyrophoric and if possible inexpensive. Finally, in some cases (e.g. for use in particle accelerators) it should also be non-magnetic and present a low photoelectric and secondary electron yield to reduce electron emission and avoid multipactoring.

All these requirements are best fulfilled by the elements of the column IV B of the periodic table, i.e. Ti, Zr, Hf. The most restrictive requirement is the high solubility limit for oxygen, which exceeds 10% for these elements only. Therefore, Ti, Zr, Hf and some of their binary combinations have been taken as an obvious starting point for the present experimental study. However, it should be noted that another family of elements, namely those of column VB (i.e. V, Nb, Ta) provide much higher oxygen diffusivity (but a low oxygen solubility limit). Therefore, elements of the IV and V columns were combined to produce the coatings studied in the second phase of this study.

## 3. Coating

Sputtering is ideally suited to this application. It is simple, applicable to a wide range of materials and alloys, of which it preserves the stoichiometry. It allows uniform and distributed coating of long, narrow vacuum chambers, and can produce alloys/compounds (and also metastable alloys which could not be obtained otherwise) by using composite cathodes.

The samples produced so far are of two distinct types. Those used for vacuum characterization are 50 cm long, 10 cm diameter internally coated stainless steel cylinders. At each coating, small size reference samples are also produced on stainless steel, copper and aluminium alloy for evaluation of thickness, adhesion, composition, film morphology and surface elemental analysis. In addition to these samples, 2–10 m long chambers of 40, 100 and 160 mm diameter have been coated for ultimate pressure and sticking coefficient evaluation (see Section 5).

A magnetron sputtering configuration has been adopted. The cathode consists of a wire (1 mm thick) of the chosen material. Alloys/compounds of variable composition are obtained by twisting together wires of different materials. The required magnetic field is produced by an external solenoid, coaxial to the cylindrical sample. All samples have been produced using the same (non-optimized) parameters, namely a magnetic field of  $\sim 100\ \text{G}$ , a cathode voltage of  $-500\ \text{V}$  (sample at ground potential), an argon pressure of  $2 \times 10^{-2}$  Torr. During coating the cathode reaches a temperature of  $\sim 1300^\circ\text{C}$  and the sample is stabilized at  $100^\circ\text{C}$ . The typical deposition rates obtained are of the order of  $1\ \text{\AA}\ \text{s}^{-1}$ , and the film thickness about  $1.5\ \mu\text{m}$ . The temperature of the cathode may

be reduced either by decreasing the sputtering rate and/or by increasing the cathode diameter. With a 10 mm diameter cathode and a deposition rate of  $1 \text{ \AA s}^{-1}$  the cathode operating temperature is of the order of  $400^\circ\text{C}$ .

The adopted magnetron sputtering configuration provides a high electron ionization efficiency (the electron path is made longer by the magnetic field), a feature which allows the argon discharge pressure to be reduced, and consequently to limit the energy loss of the sputtered atoms by gas scattering. Since excessive energy loss may endanger film adhesion, this configuration is mandatory whenever the cathode to wall distance is large (5 cm or more). At the other extreme, the magnetron configuration is also mandatory for coating tubes of very small diameter ( $\leq 20$  mm). In this case, the applied magnetic field is needed to increase the ionizing path of the electrons so as to produce enough electron multiplication to sustain the sputtering discharge.

#### 4. Characterization

During NEG activation under UHV conditions, the oxygen surface content is progressively reduced and finally reaches a minimum value when activation is completed. Therefore, surface elemental analysis is an appropriate way to monitor the activation process.

However, this technique does not provide information on the vacuum performance of the activated NEG, which therefore has to be studied by other means, namely electron stimulated desorption (ESD), ultimate pressure and pumping speed measurements. In all cases studied to date, the results obtained from these different techniques were found to be mutually consistent and displayed the relevant variation in the same range of temperatures [7].

#### 5. Experimental apparatus and results

##### 5.1. Electron stimulated desorption

For these measurements the sample (a coated stainless steel tube of 50 cm length and 10 cm diameter) is connected to a vacuum system housing an electron source which may be moved in and out of the sample by compressing or expanding long bellows. A complete description of the ESD apparatus is given in Ref. [7]. The typical ESD measuring sequence is as follows.

The sample is connected and pumped while the electron source is kept under UHV by closing a gate valve. During bakeout the sample is kept at room temperature and pumped by a turbomolecular pumping station (about  $70 \text{ l s}^{-1}$  effective speed for  $\text{H}_2$ ). At the end of the bakeout the sample is heated for 2 h at about  $100^\circ\text{C}$  and after baking a pressure in the  $10^{-10}$  Torr range is

achieved. Then the sample is heated for 2 h at a given temperature, cooled to room temperature and bombarded by electrons (energy 500 eV, current intensity 1 mA) while recording total and partial pressure variations. At the end of this operation, the electron source is retracted and isolated by closing the gate valve and the sample is heated again for 2 h at a higher temperature. The temperature increase at each step, about  $50^\circ\text{C}$ , was chosen in order to keep the effect of each heating cycle negligible with respect to that of the following.

The initial measurements, carried out on a passivated surface, provide a direct measurement of the desorption yields for all gases. However, when the NEG surface becomes progressively activated, the measured yields are in reality defined by the competing actions of surface degassing and pumping. Since the pumping speed provided by the sample depends on the impact point of the bombarding electrons, the position of the electron source is carefully reproduced for all measurements ( $170 \pm 1$  mm from sample extremity where the measuring instruments are located).

At first, samples coated with elemental Ti, Hf and Zr were produced and tested. The results are shown in Fig. 1. Titanium follows the stainless steel reference curve up to  $300^\circ\text{C}$ , and then quickly drops by two orders of magnitude at  $400^\circ\text{C}$ . Hafnium and zirconium are slightly poorer at the beginning, but activation starts at lower temperatures (about  $200^\circ\text{C}$ ) and sets in more progressively, reaching the same value as titanium at  $400^\circ\text{C}$ . The results of Fig. 1 are a clear indication that these elements are adequate for use on stainless steel

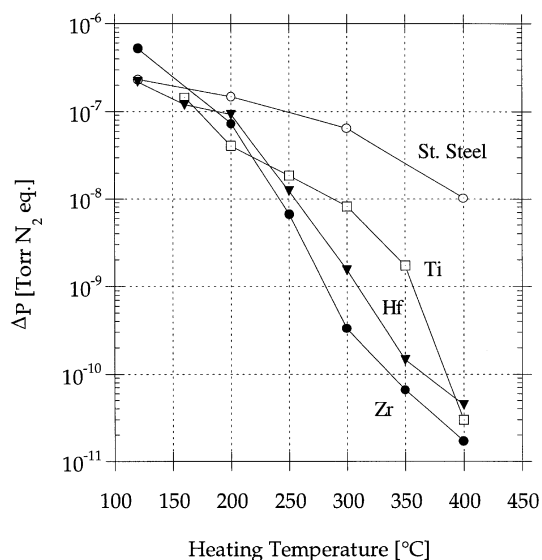


Fig. 1. Total pressure increase induced by electron bombardment of stainless steel and of coatings of Ti, Zr, Hf. The measurements are carried out at  $20^\circ\text{C}$  after sample heating for 2 h at the indicated temperatures without intermediate air venting. The electron energy is 500 eV and the electron current 1 mA.

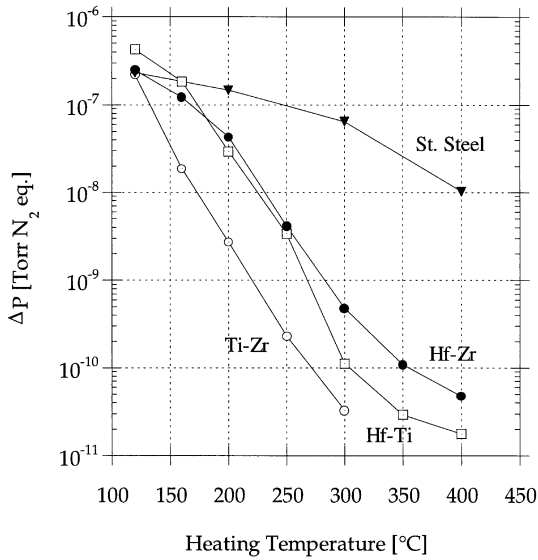


Fig. 2. Same as Fig. 1, for binary quasi-equiatomic alloys of Ti, Zr, Hf.

chambers, but completely useless if a baking temperature of 200°C cannot be exceeded, as is the case for chambers made of copper or aluminium alloys.

The results obtained on quasi-equiatomic binary Ti, Zr and Hf alloys (produced by means of composite cathodes made by intertwining two wires of different materials, both of 1 mm diameter) are given in Fig. 2. Compared to elemental coatings, the alloys display a lower activation temperature, the lowest being that of TiZr. In this case, activation starts at about 150°C and is practically completed at 300°C.

The “effective” desorption yields for the various desorbing gases are given in Fig. 3 for the quasi-equiatomic TiZr film. Note the fast decrease of CO<sub>2</sub> and the leading presence of H<sub>2</sub> at all temperatures. These features are common to all NEG coatings studied to date. Since CH<sub>4</sub> is not pumped at all by NEGs, the values given in Fig. 3 for this gas are real desorption yields and provide direct evidence of surface cleaning by heating [7].

With the aim of obtaining a further reduction of the activation temperature, Ti and Zr have been combined in different proportions by using cathodes made of one wire of an element and two wires of the other. The actual composition of the films, analysed by energy dispersive X-ray (EDX) was found to correspond closely to the macroscopic composition of the cathodes. However, this approach did not provide the benefits hoped for [7].

The study was then extended to ternary alloys based on TiZr to which a third element from the VB column of the periodic table was added. Vanadium was the first choice, the TiZrV film being produced from a cathode obtained by intertwining three elemental wires of 1 mm diameter.

The ESD performance of the TiZrV coating is compared to that of TiZr in Fig. 4. While the two coatings are

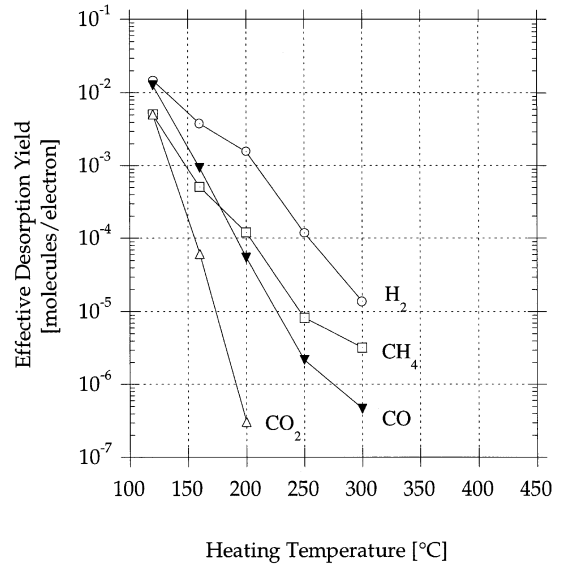


Fig. 3. Effective desorption yield of H<sub>2</sub>, CO, CO<sub>2</sub> and CH<sub>4</sub> for a quasi-equiatomic TiZr coating. The measuring conditions are the same as indicated for Fig. 1. “Effective” here indicates the net desorption per impinging electron, as resulting from the competing action of surface degassing and pumping. Since CH<sub>4</sub> is not pumped, the measurements represent a real desorption yield for this gas.

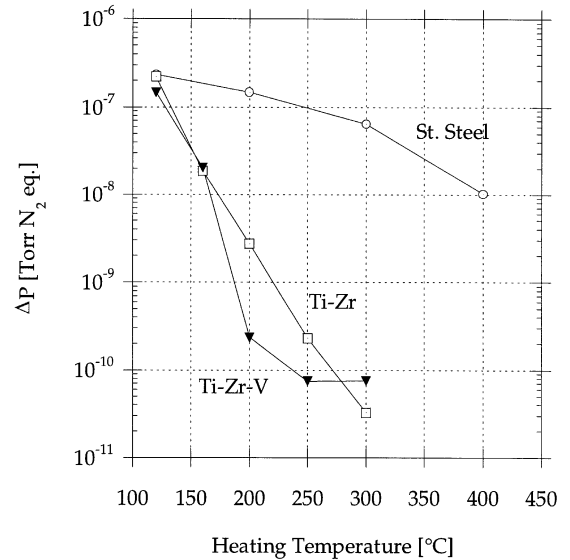


Fig. 4. Comparison of ESD measurements for stainless steel, TiZr and TiZrV coatings. Experimental conditions as described for Fig. 1.

practically equivalent initially and after full activation, the TiZrV coating displays a much faster improvement between 160 and 200°C and reaches the degassing minimum already at 250°C. Gas analysis, not presented here, indicates that all the desorbed species show a similar variation at a temperature about 50°C lower than in the case of TiZr.

The spectacular improvement with this first ternary alloy has triggered its complete characterization, and the testing of other candidates was delayed to a later date. Extending the duration of the heating cycle, as an alternative to increasing temperature, was investigated for both TiZr and TiZrV. For both these coatings a heating period of 24 h at a given temperature was found to provide the same performance as obtained when heating for 2 h at a temperature about 50°C higher [7]. This means that TiZrV coatings are fully activated by 24 h baking at 200°C.

Both coatings are quite robust with respect to ageing due to activation/air venting cycles. Five such cycles are feasible without dramatic ESD performance deterioration.

### 5.2. Ultimate pressures

Ultimate pressures were measured after baking at different temperatures in a variety of vacuum systems equipped with NEG coated chambers of different dimensions, ranging from 2 to 10 m length and from 4 to 16 cm diameter.

The difficulty of these measurements, particularly for pressures lower than  $10^{-12}$  Torr, comes from the contradictory requirements of limiting gas backstreaming from the pumps on the one hand and providing enough pumping for  $\text{CH}_4$  on the other. The first of these requirements would imply a small conductance between pumps and coated chambers, while a large conductance would be needed to pump  $\text{CH}_4$  more effectively.

The TiZr coating was studied more extensively than any other coating, with the following results. The lowest ultimate pressure, about  $7 \times 10^{-14}$  Torr, was measured, after 24 h, 350°C bakeout, at the extremity of a 2 m long, 16 cm diameter coated chamber pumped by a combination of Ti sublimation/sputter-ion pump through an orifice of  $25 \text{ l s}^{-1}$  conductance for  $\text{H}_2$  [8]. The worst possible conditions were investigated using a 10 m long, 4 cm diameter coated chamber, pumped by a sputter-ion pump of about  $20 \text{ l s}^{-1}$  effective speed. In this case, no conductance was interposed and a pressure of  $8 \times 10^{-13}$  Torr was obtained at the extremity opposite to the pump after 24 h baking at 300°C. No residual gas analyser was available to determine the causes of the pressure limitations because these instruments are usually a very important source of degassing, which may spoil the ultimate pressure to be measured. However,  $\text{CH}_4$  is probably the cause of the vacuum limitation, because the measured pressure may be calculated on the grounds of the measured  $\text{CH}_4$  outgassing and of the available pumping speed for this gas (about  $1 \text{ l s}^{-1}$  at the location of the gauge).

The comparison between the TiZr and TiZrV coatings was done using in both cases a 2 m long, 10 cm diameter chamber pumped by a Ti sublimation/sputter-ion

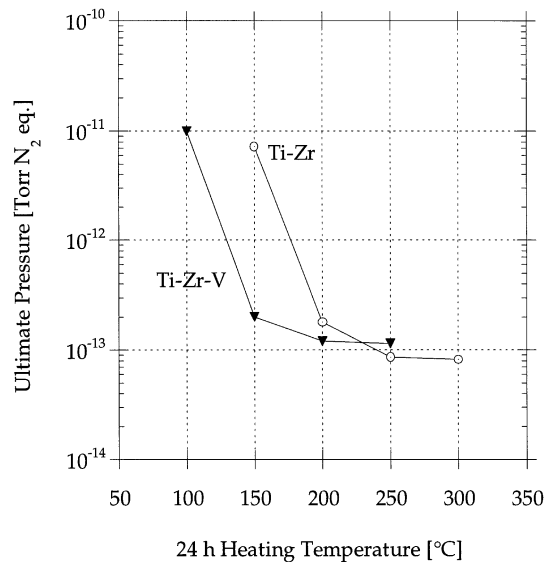


Fig. 5. Ultimate pressures obtained after 24 h baking cycles, without intermediate air venting, on chambers coated with TiZr and TiZrV. Chamber length 2 m, diameter 10 cm, applied pumping speed  $25 \text{ l s}^{-1}$  for  $\text{H}_2$ .

pumping station via an orifice of  $25 \text{ l s}^{-1}$  conductance for  $\text{H}_2$ . The results are illustrated in Fig. 5. In both cases the chambers were baked for 24 h at a given temperature, cooled to room temperature for the measurement, then heated again for 24 h at a higher temperature and so on. The temperatures were chosen so as to render the effect of a baking cycle negligible with respect to that of the following cycle. As already seen for ESD measurements, in this case also TiZrV displays activation at a temperature about 50°C lower than TiZr. A 24 h bake at 200°C is sufficient for full activation of the TiZrV coating.

### 5.3. Pumping speeds

At the end of each baking cycle, gases were injected into the pumping station to estimate the contribution of gas entering the coated chamber via the conductance orifice to the ultimate pressure measured at the opposite extremity. As a by-product of this operation, the sticking coefficients for the injected gases may be extracted from the pressure drop across the chamber by means of a Monte Carlo simulation [9]. This procedure is better suited than the methods usually employed for pumping speed measurements because it provides unrivalled sensitivities using very long chambers. For instance, making use of the 10 m long chamber described in Section 5.2, sticking coefficients as low as  $10^{-6}$  could be measured. The other obvious advantage of this procedure is that sticking coefficients and ultimate pressures are measured for the same coating conditions and no additional apparatus or measuring effort is required. The variation of the  $\text{H}_2$  sticking coefficients as a function of the 24 h baking

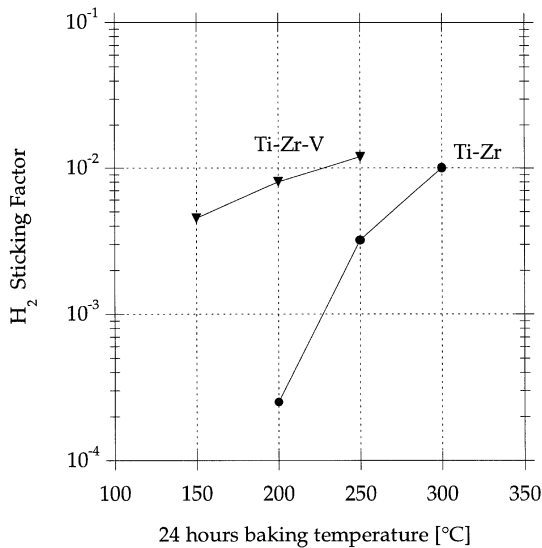


Fig. 6. Variation of the  $H_2$  sticking coefficient for TiZr and TiZrV coated chambers as a function of baking (24 h) temperature. Data obtained by gas injection and Monte Carlo simulation.

temperature is shown in Fig. 6. Here again, the lower activation temperature of TiZrV is clearly evident. In both cases the highest sticking coefficient, about  $10^{-2}$ , results in a specific pumping speed for  $H_2$  of about  $0.5 \text{ l s}^{-1} \text{ cm}^{-2}$ . The corresponding figures for CO are of the order of  $4 \text{ l s}^{-1} \text{ cm}^{-2}$ .

#### 5.4. Surface analysis

XPS measurements were performed with a SPECS EA10P hemispherical analyser using non-monochromatic Al  $K_{\alpha}$  radiation (1486.6 eV) as excitation source. Thin films of TiZr and TiZrV grown on stainless steel, copper, and aluminium substrates have been measured as-received and after an in situ thermal treatment ( $\sim 250^\circ\text{C}$  for 2 h) under UHV conditions. The reported binding energies ( $E_b$ ) are determined within an error of  $\pm 0.3 \text{ eV}$ .

Fig. 7 shows the XPS lines of the Zr 3d doublet (spin-orbit splitting) of (a) as-received TiZr, (b) TiZr after an in situ thermal cycle, and (c) TiZrV after the same thermal cycle. For as-received films,  $E_b(\text{Zr}3d_{5/2}) = 181.8 \text{ eV}$ , a value which corresponds to oxidized Zr. After the thermal treatment, a shoulder emerges at lower binding energies in (b), which is more pronounced in (c). In this latter case  $E_b(\text{Zr}3d_{5/2}) = 178.9 \text{ eV}$ , which is identified as metallic Zr [10]. This effect is more pronounced for TiZrV films, providing direct evidence of their lower activation temperature.

The same behaviour is observed for the Ti 2p lines. For the as-received (oxidized) samples  $E_b(\text{Ti}2p_{3/2}) = 458.0 \text{ eV}$ , whereas after thermal treatment the line shifts to 454.1 eV, which corresponds to metallic Ti [11].

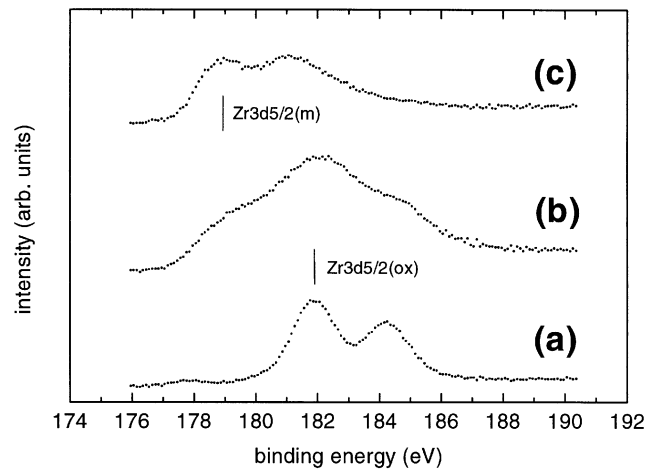


Fig. 7. XPS Zr 3d lines of (a) as-received TiZr (b) TiZr after heating 2 h at  $250^\circ\text{C}$  and (c) TiZrV after the same thermal cycle. The oxidized (ox) and metallic (m) states are indicated.

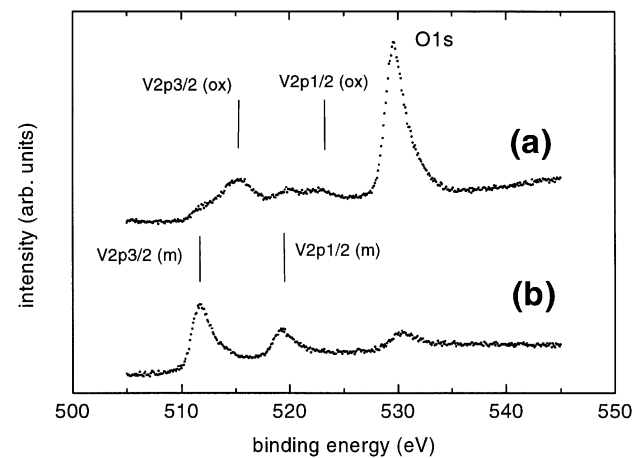


Fig. 8. XPS V 2p and O 1s lines of (a) as-received TiZrV and (b) TiZrV after heating 2 h at  $250^\circ\text{C}$ . The oxidized (ox) and metallic (m) states are indicated. The contribution of metallic V is even observed in the as-received sample. The structure between V  $2p_{3/2}$  (ox) and V  $2p_{1/2}$  (ox) is mainly due to an  $\text{AlK}_{\alpha 3}$  satellite from the O 1s line.

Fig. 8 shows the V 2p and O 1s lines of (a) as-received TiZrV and (b) TiZrV after in situ thermal cycle (2 h at  $250^\circ\text{C}$ ). In (a) the dominant O 1s peak ( $E_b = 529.7 \text{ eV}$ ), arising mainly from oxides, and a V 2p doublet ( $E_b(\text{V}2p_{3/2}) = 515.4 \text{ eV}$ ) corresponding to oxidized V are observed. After the thermal treatment (b), the O 1s signal is strongly reduced and metallic V is detected ( $E_b(\text{V}2p_{3/2}) = 512.2 \text{ eV}$ ) [10, 12]. After the thermal treatment a carbide signal at  $E_b(\text{C}1s) = 282.1 \text{ eV}$  is also observed [10].

In conclusion, after a thermal treatment under UHV conditions ( $\sim 250^\circ\text{C}$  for 2 h), the initially oxidized surfaces become metallic showing that activation has taken place. The activation process, consisting of the dissolution of oxygen into the bulk, has been studied earlier with

XPS for ZrVFe getters [12]. In the present case, the XPS analysis does not reveal any influence associated with the nature of the substrate (stainless steel, Cu or Al).

## 6. Conclusions

NEG coatings are a powerful way to achieve very low pressures, below  $10^{-13}$  Torr, inside long pipes of small diameter. After full activation they provide pumping speeds of about  $0.5 \text{ l s}^{-1} \text{ cm}^{-2}$  for  $\text{H}_2$  and  $4 \text{ l s}^{-1} \text{ cm}^{-2}$  for CO.

To date, the lowest temperature required to fully activate a NEG coating during 24 h bakeout is  $200^\circ\text{C}$ , i.e. low enough for use with Al-based vacuum chambers. However, the study of NEG coatings is still in progress and a further reduction of the activation temperature may be hoped for.

NEG coatings are quite robust with respect to activation/air venting cycles (up to 5 such cycles are possible without major performance deterioration) but this ageing process clearly represents the major weakness of this technique. While for the long vacuum systems of particle

accelerators this inconvenience may be partially circumvented by venting to inert gas before opening, it may represent an insurmountable obstacle for application to laboratory vacuum systems routinely opened to air.

## References

- [1] Benvenuti C, Hauer M. In: Proc 8th Int Vac Congr, vol. 2, Suppl à la revue "Le Vide, les couches minces". 1980;201:199.
- [2] Benvenuti C. Nucl Instr and Meth 1983;205:391.
- [3] Benvenuti C, Bojon JP, Chiggiato P, Losch G. Vacuum 1993; 44:507.
- [4] Giorgi TA. Japn J Appl Phys Suppl 1974;2:53.
- [5] Boffito C, Ferrario B, della Porta P, Rosai L. J Vac Sci Technol 1981;18:1117.
- [6] Benvenuti, C, Chiggiato P. Vacuum 1993;44:511.
- [7] Benvenuti C, Chiggiato P, Cicoira F, L'Aminot Y. J Vac Sci Technol A 1998;16:148.
- [8] Benvenuti C, Chiggiato P, Cicoira F, Ruzinov V. Vacuum 1998;50:57.
- [9] Smith CG, Lewin G. J Vac Sci Technol 1966;3:92.
- [10] Vedel I, Schlapbach L. J Vac Sci Technol A 1993;11:539.
- [11] Sullivan JL, Saied SO, Choudhury T. Vacuum 1992;43:89.
- [12] Meli F, Sheng Z, Vedel I, Schlapbach L. Vacuum 1990;41:1938.